

# THE MICROSTRUCTURAL EVOLUTION OF MICROCRYSTALLINE CELLULOSE DURING CARBONIZATION

Yo-Rhin Rhim\*, Dajie Zhang, and Dennis C. Nagle

\*Applied Physics Laboratory, Johns Hopkins University,  
Laurel, MD 20723

Advanced Technology Laboratory, Johns Hopkins University,  
Baltimore, MD 21210

## Introduction

The understanding of the structure and related property evolution during carbonization is imperative in engineering carbon materials for specific functionalities. High-purity cellulose was used as a model precursor to help understand the conversion of organic compounds to hard carbons. Several microstructural characterization techniques were employed to follow the evolution of the precursor to carbon during the heat treatment range of 250°C to 2000°C. Tools were used to characterize both long and short-range order during the carbonization of microcrystalline cellulose, including XRD, Raman, EELS, and HR-TEM analyses. These methods supported the existence of carbon clusters and indicated the mechanisms of their growth. Structural evolution was strongly correlated to changes in electrical, thermal, and chemical properties [1, 2].

## Experimental

Avicel microcrystalline cellulose powder was mechanically pressed and heat treated in an inconel-lined retort furnace with flowing argon. Samples were heat-treated to different final heat treatment temperatures (*HTTs*) and each of its microstructural properties investigated using various characterization tools.

X-ray diffraction (XRD) analysis provides information on the arrangement of atoms within a crystal. XRD patterns were collected for microcrystalline cellulose samples heat treated to several *HTTs* to characterize the crystalline phase evolution. Philips XRG3100 X-ray diffractometer operating at 35kV, 20mA, Cu-K $\alpha$  radiation was used to collect XRD patterns.

Raman spectroscopy, a technique used to measure the frequency of vibrations of chemical bonds, was also employed to observe short-range order changes during carbonization. A Horiba LabRam HR800 system with a 15 mW 633 nm He-Ne laser with excitation line set to  $\lambda_0 = 514.57$  nm and magnification set to x40 was utilized for all tests. Detailed scans from 600  $\text{cm}^{-1}$  to 2500  $\text{cm}^{-1}$  were conducted for three different spots of each sample. Grams AI software was used to analyze all spectra through background subtraction and peak fitting.

Furthermore, electron energy loss spectroscopy (EELS) was employed to determine the chemical state of each sample. Lastly, high-resolution transmission electron microscopy (HR-TEM) was used to pictorially describe the microstructural evolution of carbon clusters during the conversion of

microcrystalline cellulose to carbon with increasing *HTT*. Samples were microtomed to yield 100 nm thick shavings and placed onto holey carbon grids for both EELS and HR-TEM analysis. Spectra for samples were collected using the Philips CM300 and Gatan GIFF 200 electron spectrometer. Convergence and collection angles, were respectively set to  $\alpha = 4$  mrad and  $\beta = 15$  mrad for all samples. Polarization was not taken into effect since random orientation of crystallites was assumed.

## Results and Discussion

XRD spectra (Fig 1a) show an increase in crystallinity with increasing *HTT*. Three peaks at about 26°, 43°, and 80° are observed and correspond to the {002}, {100}, and {110} planes respectively [3]. Background noise was observed for all samples, while decreasing with rising *HTTs*. Observance of high background noise is attributable to the effects from the amorphous phase. As suspected, increases in *HTTs* lead to lower background noises and narrowing of peaks as the amorphous phase is converted to a crystalline phase.

Complementing XRD analysis, EELS reveal the conversion from an amorphous  $\text{sp}^3$  to crystalline  $\text{sp}^2$  carbon with an increase in *HTT*. Shown in Fig 1b, are the C-K edges collected for heat-treated microcrystalline cellulose. Two sharp peaks are observed at 285 eV and 295 eV denoting energy losses due to  $\pi^*$  and  $\sigma^*$  transitions. An increase in the  $\pi^*$ -peak is observed with rising *HTTs*. Furthermore, sharpening of the  $\sigma^*$ -peak and transitions related to graphitic structure [4] are observed with increases in *HTT*.

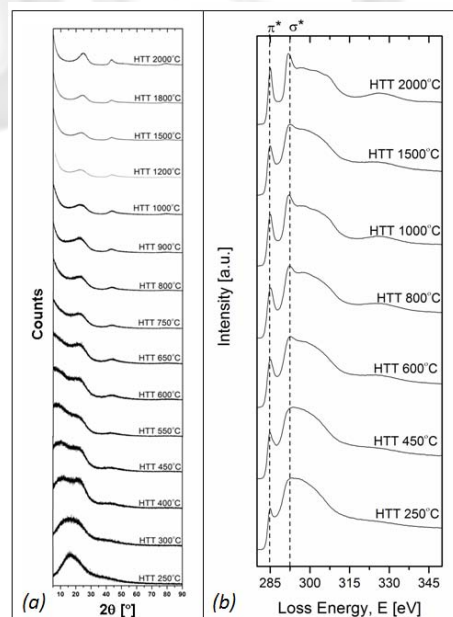


**Fig. 1** (a) XRD patterns and (b) EELS spectra for heat treated microcrystalline cellulose.

Crystalline thickness,  $L_c$ , and lateral distances,  $L_a$ , were determined by applying measured FMHM of the observed {002} and {100} peaks to Scherrer's equation and presented

in Fig. 2. Both  $L_c$  and  $L_a$  increase with higher  $HTTs$ ; however, larger variations of  $L_a$  with  $HTT$  suggest that growth in the lateral direction is predominant.

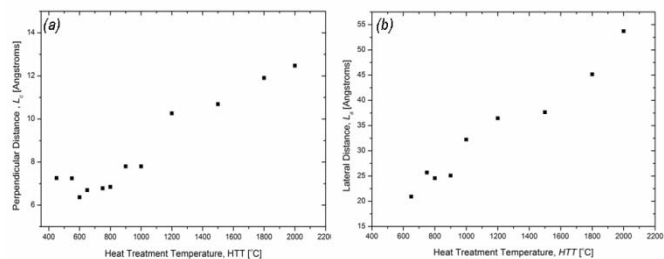


**Fig. 2.** Calculated (a) crystalline thickness,  $L_c$  and (b) lateral distances,  $L_a$ .

Raman spectra were obtained for microcrystalline cellulose samples heat-treated over the range from 250°C to 2000°C to investigate the effects of short-range order. Two main peaks located at Raman shifts of 1350  $\text{cm}^{-1}$  (D-peak) and 1575  $\text{cm}^{-1}$  (G-peak) were observed for all Raman spectra. The G-band, also previously observed for single crystal graphite, arises from the in-plane vibrations of  $\text{sp}^2$  bonded crystallite carbon [5, 6]. The ratio of the integrated areas of the D to the G-band,  $\frac{I(D)}{I(G)}$ , is inversely related to the lateral distance,  $L_a$ , of graphitic materials [5].  $\frac{I(D)}{I(G)}$  ratios were calculated all heat treated samples and results presented in Fig. 2 as a function of  $HTT$ .

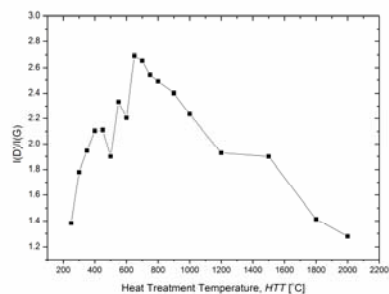


**Fig. 2**  $I(D)/I(G)$  ratios as a function of  $HTT$ .

An increase of  $\frac{I(D)}{I(G)}$  is observed as  $HTT$  increases from 300°C to 650°C due to depolymerization. For increasing  $HTTs$  between 650°C and 2000°C,  $\frac{I(D)}{I(G)}$  decreases as the disordered carbon converts to ordered  $\text{sp}^2$  carbon crystallites, resulting in increasing crystalline thickness,  $L_c$ .

Analysis of the XRD  $\{001\}$  peak and Raman  $I(D)/I(G)$  suggest that growth in the lateral direction occurred most significantly between temperatures of 600°C to 2000°C due to the conversion of amorphous  $\text{sp}^2$  phase to crystalline carbon. These carbon layers were shown to appear as curved sheets through HR-TEM analysis at 600°C and grow in both curvature and length with  $HTT$  increases of up to 2000°C (shown in Fig. 3).

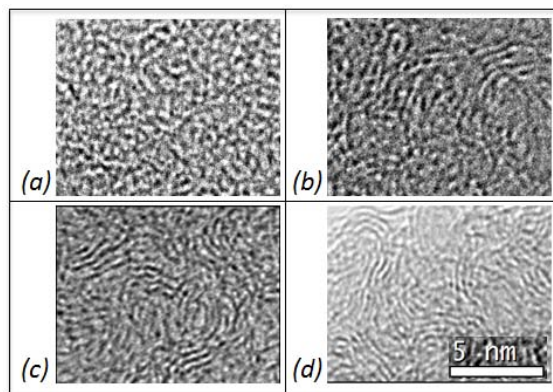


**Fig. 3** HR-TEM images of microcrystalline cellulose samples heat treated to (a) 250°C, (b) 600°C, (c) 1000°C, and (d) 2000°C.

### Conclusions

EELS, XRD, Raman, and HR-TEM analyses have been conducted to study the microstructural evolution of microcrystalline cellulose during carbonization. Such tools were used to identify carbon clusters and observe their evolution upon heat treatment. HR-TEM imaging identified carbon clusters as aggregates of curved “onion-like” carbon structures. EELS analyses show the conversion of most of the  $\text{sp}^3$  to  $\text{sp}^2$  bonds with increasing  $HTTs$ . XRD and Raman analyses provided insights to the mechanisms of carbon cluster growth. Amorphous  $\text{sp}^3$  and  $\text{sp}^2$  phases were converted to crystalline phases during heat treatment and increases in crystallinity. Growth of ordered carbon structures along the lateral direction were shown to be dominant over dimensional increases due to the stacking of carbon layers between 600°C and 2000°C.

### References

- [1] Rhim YR, Zhang D, Fairbrother DH, Wepasnick KA, Livi KJ, Bodnar RJ, et al. Changes in electrical and microstructural properties of microcrystalline cellulose as a function of carbonization temperature. *Carbon* 2010; 48(4): 1012-1024.
- [2] Rhim YR, Zhang D, Rooney M, Nagle DC, Fairbrother DH, Herman C, et al. Changes in the thermophysical properties of microcrystalline cellulose as a function of carbonization temperature. *Carbon* 2010; 48(1): 31-40.
- [3] Kercher AK, Nagle DC. Microstructural evolution during charcoal carbonization by X-ray diffraction analysis. *Carbon* 2003; 41: 15-27.
- [4] El-Barbary AA, Trasobares S, Ewels CP, Stephan O, Okotrub AV, Bulusheva LG, et al. Electron spectroscopy of carbon materials: experiment and theory. *Journal of Physics: Conference Series* 2006; 26: 149-152.
- [5] Tuinstra F, Koenig JL. Raman spectrum of graphite. *Journal of Chemical Physics* 1970; 53(3): 1126-1130.
- [6] Ferrari AC, Roberston J. Interpretation of Raman spectra of disordered and amorphous carbon. *Physical Review B* 2000; 61(20): 14095-14107.